Bottom tetraquark production at RHIC?

R. Vogt

Nuclear and Chemical Sciences Division, Lawrence Livermore National Laboratory, Livermore, California 94551, USA
and Department of Physics and Astronomy, University of California, Davis, California 95616, USA

A. Angerami

Nuclear and Chemical Sciences Division, Lawrence Livermore National Laboratory, Livermore, California 94551, USA

(Received 3 September 2021; accepted 20 October 2021; published 17 November 2021)

A resonance has been observed by the ANDY Collaboration at the Relativistic Heavy-Ion Collider at Brookhaven National Laboratory in Cu + Au collisions at center-of-mass energy $\sqrt{s} = 200$ GeV and at forward rapidity with an average mass of 18.15 GeV. The Collaboration suggests that it is a $b\bar{b}b\bar{b}$ tetraquark state decaying to two $\Upsilon(1S)$ states, each measured through the $\Upsilon \to ggg$ channel. Here, their suggestion is investigated assuming that the two Υ states are produced through the materialization of a $|uudb\bar{b}b\bar{b}\rangle$ Fock state in the projectile. The Υ pair mass and rapidity distributions arising from such a state are calculated. The production of an $X_b(b\bar{b}b\bar{b})$ tetraquark state from the same Fock configuration is also investigated. The dependence on bottom quark mass and their transverse momentum range is also studied. It is found that double Υ production from these $|uudb\bar{b}b\bar{b}\rangle$ states peak in the rapidity range of the ANDY detector. The Υ pair and X_b masses are, however, higher than the mass reported by the ANDY Collaboration. Thus the results obtained from these calculations are incompatible with the ANDY result. They are, however, compatible with previous predictions of $b\bar{b}b\bar{b}$ tetraquark masses.

DOI: 10.1103/PhysRevD.104.094025

I. INTRODUCTION

Quantum chromodynamics (QCD) is the theory describing the interactions among quarks and gluons. The fundamental color charges in this theory are confined in color-neutral objects known as baryons and mesons, containing three quarks and quark-antiquark pairs respectively. Since the advent of QCD, the existence of other, exotic, hadrons outside the conventional quark model, such as tetraquarks and pentaquarks, consisting of four or five valence quarks respectively, have been postulated, as early as in Murray Gell-Mann's introduction of the quark model [1].

Most exotic hadrons so far discovered contain at least one $c\bar{c}$ pair. The first proposed tetraquark candidate, the $X(3872)$, measured by Belle [2] in e^+e^- collisions, has been observed in many systems, including in nucleus-nucleus collisions [3]. The $Z(4430)$, a $c\bar{c}d\bar{u}$ tetraquark candidate was first measured by Belle [4] and later confirmed by LHCb [5]. The $Z(3900)$, reported by BES III [6] and Belle [7], was confirmed as a four-quark state. Most recently, LHCb announced the discovery of a $c\bar{c}c\bar{c}$ tetraquark, the $X(6900)$ [8]. LHCb has also announced the discovery of a $uudc\bar{c}$ pentaquark state, the $P_c(4312)^+$ [9]. The Belle Collaboration presented discovery of two $b\bar{q}\,\bar{q}$ states decaying to a pair of B mesons, $Z_b(10610)$ and $Z_b(10650)$ [10]. So far no tetraquark states containing four b quarks, $b\bar{b}b\bar{b}$, have been confirmed.

The ANDY Collaboration has recently reported an observation of a resonance with a mass of 18.15 GeV in Cu + Au collisions at the Relativistic Heavy-Ion Collider (RHIC) [11]. This observation was made at forward rapidity and was interpreted as a $b\bar{b}b\bar{b}$ tetraquark state decaying to two $\Upsilon(1S)$ states, each decaying to hadrons through the $\Upsilon \to ggg$ channel. These data were taken at $\sqrt{s_{NN}} = 200$ GeV in 2012. They used a minimum bias trigger plus an inclusive jet and dijet trigger. Because no luminosity measurement was performed, the results were presented as fractions of the minimum bias yields.

In that analysis, multiple jets were found in a given event. Through an event-mixing study they found that only high energy dijets exhibited azimuthal angular correlations. No such correlations were observed for low energy dijets. They constructed the dijet mass for these large energy dijets and found peaks at $M_{\text{dijet}} = 17.83 \pm 0.2$ GeV

for dijets with energy $250 < E < 260$ GeV and at $M_{\rm dijet} = 18.47 \pm 0.22$ GeV for dijets with energy $260 < E < 270$ GeV. Both peaks have high statistical significance, 9σ and 8.4σ respectively, since there is little background in this region. Combining the two dijet energy bins gives an average dijet mass of $M_{\rm dijet} = 18.12 \pm 0.15$ GeV. The two jets comprising the dijet were measured within the calorimeter acceptance $3.0 < \eta < 3.5$ [11]. They then looked for candidate $\Upsilon(1S)$ decays to three gluons and found evidence for double Υ production, both of which decayed hadronically through $\Upsilon(1S) \to 3g$. They concluded that the best candidate for their dijet mass signal is a $X_b(b\bar{b}b\bar{b})$ tetraquark state.

The authors of Ref. [11] noted that there have been many predictions of an X_b tetraquark mass, all of them larger than the ANDY value of 18.12 GeV. Karliner, Rosner and Nussinov [12] obtained a mass of 18.826 GeV based on meson and baryon mass systematics. A similar mass value, 18.84 ± 0.09 GeV, was found by Wang [13], based on QCD sum rules. Calculations of the ground state X_b mass by Bai, Lu and Osborne [14] and Wu *et al.* [15] found lighter masses of 18.69 GeV and 18.46 GeV respectively. Other calculations of $b\bar{b}b\bar{b}$ tetraquark states [16,17] predict $\Upsilon(1S)\Upsilon(1S)$ tetraquark states with $J^{PC} = 1^{+-}$ with masses of $\approx$19 GeV, well above the ANDY mass but compatible with the calculations of Refs. [12,13]. Lattice QCD calculations [18], on the other hand, found no evidence for the all b tetraquark while an analysis by Richard, Valcarce and Vijande [19] suggested that such a state wound be unbound.

Experimental searches for X_b tetraquarks have been carried out in $p+p$ collisions at the LHC. LHCb set limits on the X_b mass through $\Upsilon(1S) + \Upsilon^\star \to \mu^+\mu^-\mu^+\mu^-$ in the rapidity range $2 < \eta < 5$ in $p+p$ collisions at $\sqrt{s} = 7$, 8, and 13 TeV [20]. They found no candidate events in the mass range $17.5 < M_{X_b} < 20$ GeV. CMS studied $\Upsilon(1S) + \Upsilon^\star \to \mu^+\mu^-\mu^+\mu^-$ and $\mu^+\mu^-e^+e^-$ at midrapidity in $p+p$ collisions at $\sqrt{s} = 13$ TeV [21]. They saw no evidence of a signal in the mass range $17.5 < M_{X_b} < 19.5$ GeV [21].

Pair production of quarkonium has been measured before, most recently at collider energies. For example, in the same analysis that set limits on X_b production at $\sqrt{s} = 13$ TeV, the CMS Collaboration measured double $\Upsilon(1S)$ production through both single and double parton scattering [21].

The LHCb Collaboration reported J/ψ pair production originating from $b\bar{b}$ pair production, followed by the decay of both b hadrons to J/ψ [22]. This LHCb measurement, performed in $p+p$ collisions at $\sqrt{s} = 7$ and 8 TeV, at forward rapidity, $2.5 < y < 5$, can be well described by calculations assuming that the production originates from a single $b\bar{b}$ pair [22,23]. The predominant $b\bar{b}$ production mechanism in $p+p$ collisions, perturbative QCD, produces single $b\bar{b}$ pairs at $y = 0$. The LHCb rapidity range is not far forward relative to the fractional momentum carried by the gluons initiating the $b\bar{b}$ production.

The Υ pair production suggested by ANDY, on the other hand, is in a kinematic region more similar to fixed-target J/ψ pair production measured by NA3 with π^- beams of laboratory momenta 150 and 280 GeV/c [24] and 400 GeV/c proton beams [25]. The fraction of the π^- momentum carried by the J/ψ pair in $\pi^- N \to J/\psi J/\psi X$ events was $x_{\psi\psi} \geq 0.6$ at 150 GeV/c and $x_{\psi\psi} \geq 0.4$ at 280 GeV/c. In perturbative QCD, J/ψ pair production is near $x_{\psi\psi} \sim 0$.

The average invariant mass of the $J/\psi J/\psi$ pairs measured by NA3 was well above the $2m_\psi$ threshold while the average transverse momentum of the pair was small, suggesting tightly correlated production [24,25]. These measurements were studied within the intrinsic charm model, assuming production from six and seven-particle Fock states, $|\bar{u}dc\bar{c}c\bar{c}\rangle$ and $|uudc\bar{c}c\bar{c}\rangle$ respectively, in Ref. [26]. Good agreement of the calculations with the measured mass distributions was found. Other mechanisms for double J/ψ production were further studied in Ref. [27], none of which resulted in similarly good agreement with the NA3 data.

The possibility of double Υ production from a similar Fock state would be even more rare assuming intrinsic heavy flavor production scales as $(m_c^2/m_b^2)^2$ for the production of two $Q\bar{Q}$ pairs in the same Fock state [26]. The higher energies at RHIC allow production of these more massive states.

This work investigates the ANDY result assuming that it could arise from direct $\Upsilon(1S)$ pair production or from production of an $X_b(b\bar{b}b\bar{b})$ state in QCD, assuming they arise from intrinsic heavy quark Fock states [28,29]. Both potential production channels are assumed to be produced from a single Fock state of the nucleon, in particular $|uudb\bar{b}b\bar{b}\rangle$, in a single interaction, i.e., double parton scattering is not considered. Intrinsic heavy quark states are an especially attractive candidate for the ANDY signal because they are manifested at large Feynman x instead of at central rapidities, as in the case of perturbative production. However, the ANDY detector at RHIC covers the more forward region in pseudorapidity $3 < \eta < 3.5$, larger rapidity than covered by previous measurements of heavy flavor at RHIC.

Here double Υ and $X_b(b\bar{b}b\bar{b})$ production is calculated through the materialization of double intrinsic $b\bar{b}$ Fock components of the nucleons. Note that even though the light quark content of the projectile can make a difference in which open heavy flavor states are most likely to be produced [30–32], quarkonium states such as J/ψ and Υ share no valence quarks with the colliding beams and would thus be equally produced by protons and neutrons, i.e., they are not leading particles.

Single Υ production from a $|uudb\bar{b}\rangle$ state is first described in Sec. II A. Next, Υ pair production from a $|uudb\bar{b}b\bar{b}\rangle$ state is described in Sec. II B. The Feynman-x, rapidity and pair mass distributions are calculated. The dependence of the mass distributions on the b quark mass and internal k_T dynamics of the quarks in the Fock state are shown. The possibility that the state is manifested instead as an X_b tetraquark is discussed and these distributions compared and contrasted to those for double Υ production in Sec. II C. The results are related to the ANDY kinematics. Conclusions are drawn in Sec. III.

II. INTRINSIC HEAVY FLAVOR PRODUCTION

The wave function of a proton in QCD can be represented as a superposition of Fock state fluctuations of the $|uud\rangle$ state, e.g., $|uudg\rangle$, $|uudq\bar{q}\rangle$, $|uudQ\bar{Q}\rangle$, …. When the projectile scatters in the target, the coherence of the Fock components is broken and the fluctuations can hadronize [28,29,33]. These intrinsic $Q\bar{Q}$ Fock states are dominated by configurations with equal rapidity constituents, so that the intrinsic heavy quarks carry a large fraction of the projectile momentum [28,29]. Heavy quark hadrons can be formed by coalescence, either with light quarks, e.g., to form a $\Lambda_c^+(udc)$ and $D^0(u\bar{c})$ from a $|uudc\bar{c}\rangle$ state or a final-state J/ψ with a proton. Leading charm asymmetries have been measured as a function of x_F and p_T in fixed-target $\pi^- + p$ interactions where a $D^-(d\bar{c})$, which can be produced from a $|\bar{u}dc\bar{c}\rangle$ Fock state of the negative pion, is leading over a $D^+(\bar{d}c)$ which is not [31]. It is worth noting that both D^+ and D^- can be produced at higher x_F than purely perturbative production in a higher Fock state, namely a six-particle $|\bar{u}dd\bar{d}c\bar{c}\rangle$ state, but there would be no difference in their distributions, neither would lead the other when produced from this state. In addition, the average x_F for D mesons hadronized from this state would be lower than the D^- average x_F from the minimal Fock state required to produce it, the four-particle $|\bar{u}dc\bar{c}\rangle$ state [32]. These higher Fock states would also have lower probabilities for manifestation from the projectile hadron.

In this work, the formulation for intrinsic heavy quarks in the proton wave function postulated by Brodsky and collaborators in Refs. [28,29] has been adapted. That work was more specifically directed toward charm quarks. There are also other variants of intrinsic charm distributions in the proton, including meson-cloud models where the proton fluctuates into a $\bar{D}(u\bar{c})\Lambda_c(udc)$ state [34–37], also resulting in forward production, or a sea-like distribution [38,39], only enhancing the distributions produced by massless parton splitting functions as in DGLAP evolution. Intrinsic charm has also been included in global analyses of the parton densities [38–42]. (See Ref. [43] for a discussion of a possible kinematic constraint on intrinsic charm in deep-inelastic scattering.)

The probability of intrinsic charm production, $P^0_{\rm ic5}$, obtained from these analyses, as well as others, has been suggested to be between 0.1% and 1%. The reviews in Refs. [44,45] describe the global analyses and other applications of intrinsic heavy quark states. New evidence for a finite charm quark asymmetry in the nucleon wave function from lattice gauge theory, consistent with intrinsic charm, was presented in Ref. [46].

The general consensus is that the probability of intrinsic bottom production, $P^0_{\rm ib5}$, will scale as the square of the quark mass, m_c^2/m_b^2, for production from a minimal Fock state configuration such as $|uudQ\bar{Q}\rangle$ where $Q = c$, b. A few calculations of intrinsic bottom production have been made previously [47,48]. Some additional prior results are also summarized in Ref. [44].

Here single Υ production from such a minimal Fock state configuration is summarized first with differences between results for charm and bottom highlighted. Starting from this baseline, single and double Υ production from the minimal Fock state configuration for Υ pair production, $|uudb\bar{b}b\bar{b}\rangle$, is developed. The x_F and rapidity distributions are described and the Υ pair mass distributions are presented and the sensitivities of these distributions to calculational inputs are discussed. Some attention is paid to the normalized cross section for such states but the main focus of the discussion is whether the distributions produced in this approach are compatible with the kinematic range of the ANDY measurement and, if so, are the resulting mass distributions at all compatible with their measured mass.

A. Single Υ production from a $|uudb\bar{b}\rangle$ state

Production of a single Υ from a five-particle proton Fock state is considered first, analogous to J/ψ production from such a state, as recently studied in Ref. [49]. In the case of Υ production, the frame-independent probability distribution of a 5-particle $b\bar{b}$ Fock state in the proton is

$$dP_{\rm ib5} = P^0_{\rm ib5} N_5 \int dx_1 \cdots dx_5 \int dk_{x1} \cdots dk_{x5} \int dk_{y1} \cdots dk_{y5} \frac{\delta(1-\sum_{i=1}^5 x_i)\delta(\sum_{i=1}^5 k_{xi})\delta(\sum_{i=1}^5 k_{yi})}{(m_p^2 - \sum_{i=1}^5 (m_{Ti}^2/x_i))^2}, \tag{1}$$

where $i = 1$, 2, 3 are the interchangeable light quarks (u, u, d) and $i = 4$ and 5 are the b and $\bar{b}$ quarks respectively. Here N_5 normalizes the $|uudb\bar{b}\rangle$ probability to unity and $P^0_{\rm ib5}$ scales the unit-normalized probability to the assumed intrinsic bottom content of the proton. The delta functions conserve longitudinal (z) and transverse (x and y) momentum. The denominator of Eq. (1) is minimized when the heaviest constituents carry the largest fraction of the longitudinal momentum, $\langle x_b \rangle > \langle x_q \rangle$. Given that $m_Q \gg m_q$, one does not expect large differences

between $\langle x_b \rangle$ and $\langle x_c \rangle$ from $|uudb\bar{b}\rangle$ and $|uudc\bar{c}\rangle$ states respectively.

In Ref. [49], the $J/\psi\, p_T$ distribution from intrinsic charm was calculated for the first time by integrating over the light and charm quark k_T ranges in Eq. (1). In that work, $k_{Tq}^{\rm max}$ was set to 0.2 GeV while the default for $k_{Tc}^{\rm max}$ was taken to be 1 GeV. The sensitivity of the results to the k_T integration range was tested by multiplying the maximum of the respective k_T ranges by 0.5 and 2 respectively.

In previous estimates of intrinsic bottom production where the mass distributions were not calculated, average values for the transverse masses of the constituent quarks, $m_{Ti}^2 = m_i^2 + k_{Ti}^2$, $m_{Tq} = 0.45$ GeV and $m_{Tb} = 4.6$ GeV were chosen [48]. The same procedure can be employed here for the Υ x_F distribution which is independent of the exact value of m_b chosen. Thus the x_F distribution can be calculated assuming simple coalescence of the b and $\bar{b}$ in a single state, represented in Eq. (1) by the addition of a delta function, $\delta(x_F - x_4 - x_5)$, in the longitudinal direction, ignoring the k_T integrations where 4 and 5 represent the b and $\bar{b}$ quarks. When the transverse directions are also included, employing $\delta(k_{x\Upsilon} - k_{x4} - k_{x5})$ and $\delta(k_{y\Upsilon} - k_{y4} - k_{y5})$, the x_F distribution is found to be independent of the k_T integration range.

Figure 1 shows the x distribution of a single b quark (dashed curve) and the x_F distribution of a single Υ (solid curve) from a five-particle proton Fock state. Such a calculation provides a check against previous results on the J/ψ. The average x of the b quark is 0.36 from a five-particle Fock state while the average x of a c quark is 0.34.

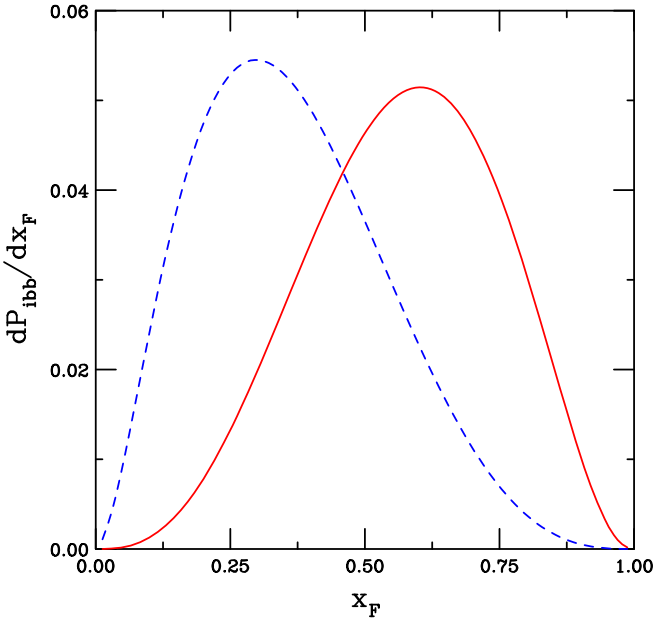

FIG. 1. The probability distribution as a function of x for a single b quark (dashed blue curve) and as a function of x_F for a single Υ (solid red curve) from a five-particle Fock state of the proton. Both curves are normalized to unity.

Because the c and b quarks are both much more massive than the light quarks in the state, there is very little difference in the average longitudinal momentum carried by the heavy quarks.

The Υ x_F distribution has an average x_F of 0.57, somewhat less than twice the average x of the b quark. This average is 7.5% larger than the average x_F of the J/ψ from a similar five-particle proton Fock state. The x_F dependence is effectively independent of the chosen k_T limits, as shown in for single J/ψ production from a $|uudc\bar{c}\rangle$ state in Ref. [49].

Following the intrinsic charm cross section calculation in Ref. [49], the intrinsic bottom cross section from a $|uudb\bar{b}\rangle$ component of the proton can be written as

$$\sigma_{\rm ib\,5}(pp) = P^0_{\rm ib5}\sigma^{\rm in}_{pN}\frac{\mu^2}{4m_{Tb}^2}. \tag{2}$$

The factor of $\mu^2/4m_{Tb}^2$ arises from the soft interaction which breaks the coherence of the Fock state. The scale $\mu^2 = 0.1$ GeV^2 is assumed for better agreement with the $J/\psi A$ dependence, see Ref. [50]. An inelastic $p + N$ cross section of $\sigma^{\rm in}_{pN} = 42$ mb is appropriate for RHIC energies.

The Υ cross section can be obtained from Eq. (2) analogously to how the cross section is obtained in perturbative QCD using the color evaporation model (CEM) which relates the $Q\bar{Q}$ cross section to the quarkonium cross sections. The same factor, $F_B = 0.022$, determined from recent CEM calculations [51] for inclusive prompt Υ production, is used here to relate the intrinsic bottom cross section to the Υ cross section from the same state,

$$\sigma^{\Upsilon}_{\rm ib5}(pp) = F_B\sigma_{\rm ib5}(pp). \tag{3}$$

The nuclear dependence of the intrinsic bottom contribution is assumed to be the same as that extracted for the nuclear surface-like component of J/ψ dependence by the NA3 Collaboration [52],

$$\sigma^{\Upsilon}_{\rm ib5}(pA) = \sigma^{\Upsilon}_{\rm ib5}(pp)A^{\beta} \tag{4}$$

with $\beta = 0.71$ [52] for a proton beam. In that experiment, two contributions to the cross section were separated, a volume-type component, with a close-to-linear nuclear dependence, and the diffractive component, associated with intrinsic charm in Ref. [50], with the A dependence given in Eq. (4) above. The A dependence here is similar to what one would expect if the incident proton interacted with the nuclear surface acting as a black disc, $A^{2/3}$ [50,52]. Note that the nuclear modification only affects the total rate, not the kinematic distributions.

Recall that the nuclear mass dependence in Eq. (4) was determined from fixed-target proton-nucleus interactions. The ANDY data were taken in Cu + Au collisions where

any nucleon in either beam could fluctuate into an intrinsic bottom Fock state and be brought on shell by a soft gluon from the opposite beam.

When generalizing Eq. (4) to nucleus-nucleus collisions, the nuclear dependence becomes more complicated. However, there is no reason to expect the Υ pair cross sections to be the same whether A_p or A_t is acting as the projectile. Naive estimates using a Glauber model yield a rate roughly 2.5 times larger in the Au-going direction than in the Cu-going direction. This suggests that performing the ANDY analysis separately for each beam configuration could provide further insight into the production mechanism.

Thus if A_p is the mass number of one nuclear beam and A_t is its oppositely-directed collision partner, the nuclear dependence for an $A_p + A_t$ collision would be

$$\sigma^{\Upsilon}_{\rm ib5}(A_pA_t) = \sigma^{\Upsilon}_{\rm ib5}(pp)A_p^{\beta_p}A_t^{\beta_t} \tag{5}$$

where the projectile and target nuclei could each have a different effective exponent, β_p and β_t respectively. The two contributions to the NA3 J/ψ production data, the hard scattering contribution with a volume-type, near linear A dependence, and the diffractive surface-type black disc contribution, are summed for the total J/ψ production cross section [52]. In $p + A$ collisions, one can define a nuclear suppression factor by dividing the summed contributions by A [49]. Similarly here a suppression factor in $A_p + A_t$ collisions can be calculated by dividing the contributions to Υ production from the hard and diffractive parts by the nuclear overlap function, $T(A_pA_t)$, and the production cross section in $p + p$ collisions [51]. Note that the focus here is only on intrinsic bottom production, hard scattering Υ production in perturbative QCD has been calculated previously and is centered at midrapidity.

The probability for intrinsic bottom production from a $|uudb\bar{b}\rangle$ state can be assumed to scale with the square of the quark mass relative to the intrinsic charm probability,

$$P^0_{\rm ib5} = P^0_{\rm ic5}\left(\frac{m_c^2}{m_b^2}\right). \tag{6}$$

In Ref. [49], the range $0.1\% \le P^0_{\rm ic5} \le 1\%$ was studied. Assuming this range, $P^0_{\rm ib5} \approx 0.075P^0_{\rm ic5}$ for $m_c = 1.27$ GeV [53] with $m_b = 4.65$ GeV, the 1S value of the bottom quark mass [54]. Employing this mass value gives $0.008\% \le P^0_{\rm ib5} \le 0.08\%$. Choosing a lower bottom quark mass would increase the probability for intrinsic bottom production in the five-particle Fock state.

Given this probability in Eq. (2), the intrinsic bottom cross section in this state, $\sigma_{\rm ib5}(pp)$, is in the range 3.6–36 nb for $m_b = 4.65$ GeV. Taking a lower value of the bottom quark mass in the calculation of $\sigma_{\rm ib5}(pp)$ would increase the cross section as well since m_b is a factor in both $P^0_{\rm ib5}$ and the factor $\mu^2/(4m_{Tb}^2)$ in Eq. (2). The total $b\bar{b}$ production cross section at next-to-leading order in perturbative QCD is 2100^{+400}_{-300} nb [55]. The scale factor for Υ production in next-to-leading order perturbative QCD is assumed to be the same for Υ production from the five-particle intrinsic bottom Fock state. Thus the difference in cross sections for Υ production in the two processes remains similar for Υ production relative to the total $b\bar{b}$ cross section. It is, however, worth noting that the Υ rapidity distribution from intrinsic bottom has its maximum where the Υ cross section calculated in perturbative QCD is steeply falling. Thus, at forward rapidity, the Υ cross section from intrinsic bottom could be comparable to or larger than the perturbative QCD cross section.

B. Double Υ production from a $|uudb\bar{b}b\bar{b}\rangle$ state

All the calculations in this section assume production of one or two Υs from a seven-particle Fock state in a proton, $|uudb\bar{b}b\bar{b}\rangle$. Building on the distributions from a five-particle Fock state in Eq. (1), the frame-independent probability distribution of a 7-particle $b\bar{b}$ Fock state in the proton is

$$dP_{\rm ibb7} = P^0_{\rm ibb7}N_7 \int dx_1 \cdots dx_7 \int dk_{x1} \cdots dk_{x7} \int dk_{y1} \cdots dk_{y7} \frac{\delta(1 - \sum_{i=1}^7 x_i)\delta(\sum_{i=1}^7 k_{xi})\delta(\sum_{i=1}^7 k_{yi})}{(m_p^2 - \sum_{i=1}^7 (m_{Ti}^2/x_i))^2}, \tag{7}$$

where $i = 1, 2, 3$ are the interchangeable light quarks (u, u, d) and $i = 4$–7 are the b and $\bar{b}$ quarks respectively. Here N_7 normalizes the $|uudb\bar{b}b\bar{b}\rangle$ probability to unity and $P^0_{\rm ibb7}$ scales the unit-normalized distribution to the assumed probability for production of this state.

The bottom quark mass, $m_b = 4.65$ GeV, used for the cross section estimates in the previous section, is the 1S bottom mass [54]. The mass threshold for the double Υ or $b\bar{b}b\bar{b}$ state is $4m_b$ with no internal k_T of the quarks in the state. Employing the 1S bottom mass, $m_b = 4.65$ GeV, the mass threshold is $4m_b = 18.60$ GeV, greater than the average ANDY mass. Therefore, a lower limit on m_b of 4 GeV is also used. This value, 4.5% below the running $\overline{\rm MS}$ bottom mass of 4.18 ± 0.03 GeV [54], allows for a lower mass threshold potentially consistent with the ANDY measurement and the predicted tetraquark masses. In this case, $0.01\% \le P^0_{\rm ib5} \le 0.1\%$

The cross section for Υ pair production from an intrinsic $|uudb\bar{b}b\bar{b}\rangle$ Fock state can determined analogously to Eq. (3), but now for two $b\bar{b}$ pairs,

$$\sigma^{\Upsilon\Upsilon}_{\rm ibb7}(pp) = F_B^2\sigma_{\rm ibb7}(pp). \tag{8}$$

Equation (2) can similarly be generalized, assuming that no additional soft scale factor of $\mu^2/4\hat{m}_b^2$ is needed for the

second $b\bar{b}$ pair in the state, as assumed in Ref. [26], giving $\sigma_{\rm ibb7}(pp) = P^0_{\rm ibb7}[\sigma^{\rm inel}_{pN}(\mu^2/4\hat{m}_b^2)]$. Using Eq. (2), the term in brackets can be rewritten as $\sigma_{\rm ib5}/P^0_{\rm ib5}$ so that, after substitution into Eq. (8), one has

$$\sigma^{\Upsilon\Upsilon}_{\rm ibb7}(pp) = F_B^2 \frac{P^0_{\rm ibb7}}{P^0_{\rm ib5}} \sigma_{\rm ib5}(pp) = F_B \frac{P^0_{\rm ibb7}}{P^0_{\rm ib5}} \sigma^{\Upsilon}_{\rm ib5}(pp) \tag{9}$$

If, $P^0_{\rm ibb7}$ scale as the mass squared relative to $P^0_{\rm icc7}$, as in Eq. (6), then

$$P^0_{\rm ibb7} = P^0_{\rm icc7}\left(\frac{m_c^2}{m_b^2}\right)^2, \tag{10}$$

this time with an additional power of the mass ratio squared for the second $Q\bar{Q}$ pair in the Fock state. In Ref. [26], $P^0_{\rm icc7} \approx 4.4\% P^0_{\rm ic5}$, based on the forward double J/ψ cross section measured by NA3 [24]. Thus $2.0\times10^{-4} P^0_{\rm ic5} \le P^0_{\rm ibb7} \le 4.5\times10^{-4} P^0_{\rm ic5}$ with the lower limit obtained for $m_b = 4.65$ GeV and the higher limit for $m_b = 4$ GeV. Taking the higher value gives $4.5\times10^{-5}\% \le P^0_{\rm ibb7} \le 4.5\times10^{-4}\%$, resulting in a small expected rate.

Following Eq. (5), one can write the $A_p + A_t$ dependence of the double Υ cross section as

$$\sigma^{\Upsilon\Upsilon}_{\rm ibb7}(A_pA_t) = \sigma^{\Upsilon\Upsilon}_{\rm ibb7}(pp) A_p^{\beta_p} A_t^{\beta_t}. \tag{11}$$

Because of the limitations in the result provided by the ANDY Collaboration, which does not report an absolute rate, further quantitative comparisons cannot be performed. The remainder of this section is thus devoted to calculations of the Υ pair x_F and rapidity distributions in Sec. II B 1 and the pair mass distributions in Sec. II B 2. The goal here is to determine whether such a $|uudb\bar{b}b\bar{b}\rangle$ state, producing either an Υ pair or an $X_b(b\bar{b}b\bar{b})$ would be compatible with the ANDY observation, without regard to the total rate.

1. x_F and rapidity distributions of Υ pair production

The x_F distribution for a single Υ from a seven-particle state can be calculated by introducing delta functions required to coalesce one of the $b\bar{b}$ pairs in the state into an Υ, $\delta(x_{\Upsilon 1} - x_{b1} - x_{\bar{b}1})$, to the probability distribution given in Eq. (7). Here the subscript "1" simply denotes one of the two $b\bar{b}$ pairs in the state. It is worth noting that there is nothing to prevent the Υ from being produced by the b quark from pair 1 and the $\bar{b}$ quark from pair 2 (and equally likely for the b quark from pair 2 to coalesce with the $\bar{b}$ quark from pair 1) since both pairs are comoving in the state. Similar delta functions can be applied to the transverse directions. Such cross coalescence can add a combinatorial factor to the probability but will not affect the shape of the distributions.

Employing a seven-particle $|uudb\bar{b}b\bar{b}\rangle$ Fock state to allow for double Υ production, one can expect the average x_F of a single Υ to be considerably reduced since the bulk

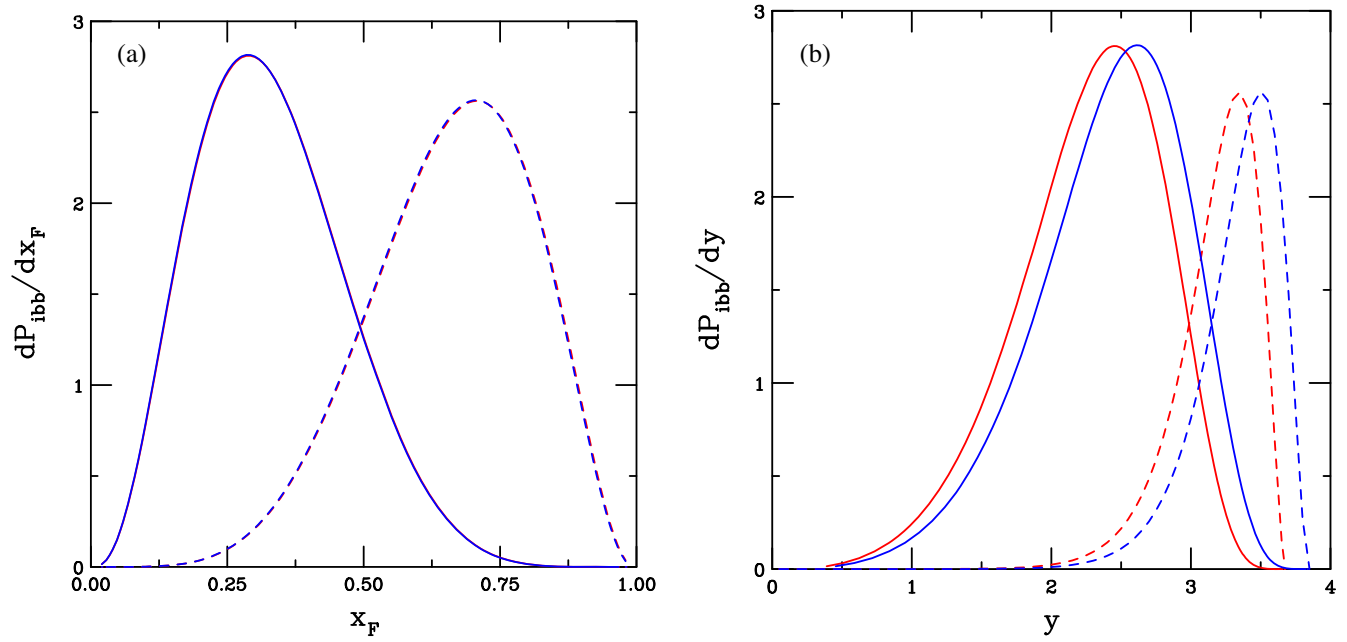

FIG. 2. The probability distributions for a single Υ state and Υ pairs from a seven-particle proton Fock state as a function of x_F (a) and rapidity (b). The solid curves show the single Υ production from the state while the dashed curves illustrate the Υ pair distributions. The red curves employ $m_b = 4.65$ GeV while the blue curves display the results for $m_b = 4$ GeV. The results are independent of the k_T integration range for the light and bottom quarks. The x_F distributions in (a) are independent of the bottom quark mass while the rapidity distributions exhibit an m_b dependence, as illustrated in (b). All curves are normalized to unity.

of the momentum has to now be distributed among four bottom quarks. As shown in Fig. 2(a), the single Υ x_F distribution from this state has an average x_F of 0.33, somewhat less than the average momentum fraction of a single b quark from a five-particle Fock state, 0.36, as shown in Fig. 1.

The x_F distribution for a pair of Υs from the same Fock state can be obtained by adding three longitudinal delta functions, $\delta(x_{\Upsilon\Upsilon} - x_{\Upsilon 1} - x_{\Upsilon 2})\delta(x_{\Upsilon 1} - x_4 - x_5)\delta(x_{\Upsilon 2} - x_6 - x_7)$, as well as those in the corresponding transverse directions to Eq. (7). Note again that the b and $\bar{b}$ that coalesce into an Υ do not have to come from the same pair since both pairs are comoving at similar velocities in the state. The Υ pair x_F distribution is shown in the dashed curve of Fig. 2(a). The average x_F of the Υ pair is double that of a single Υ state, 0.66.

Both of these distributions, the single Υ and the Υ pair, are independent of the k_T range of integration as well as the b quark mass employed. Curves with different limits of k_T integration and values of m_B are superimposed in the figure.

Since the ANDY Collaboration observed their signal at forward rapidity, Fig. 2(b) shows the same distributions as in Fig. 2(a) but now as a function of rapidity. Although the results are still independent of the k_T integration range, now there is a separation between peaks for different bottom quark masses with the distribution for the lighter bottom quark mass, 4 GeV, peaking at higher rapidity than for $m_b = 4.65$ GeV by ≈ 0.15 units of rapidity, $\langle y_\Upsilon \rangle = 2.26$ and 2.41, respectively. It can also be seen that the relatively large difference between the single and double Υ distributions as a function of x_F is reduced when the distributions are viewed as a function of rapidity. The average Υ pair rapidity distribution is ≈ 0.9 units of rapidity greater than that for a single Υ when the single Υ arises from a seven-particle Fock state. The averages are $\langle y_{\Upsilon\Upsilon} \rangle = 3.17$ and 3.33 respectively. Thus the peak of the double Υ rapidity distribution is within the range of the ANDY measurement.

2. Υ pair mass distributions

The Υ pair mass distribution predicted from a $|uudb\bar{b}b\bar{b}\rangle$ Fock state is

$$\begin{aligned}\frac{dP_{\rm ibb7}}{dM^2_{\Upsilon\Upsilon}} = &\int \frac{dx_{\Upsilon_j}}{x_{\Upsilon_j}}\frac{dx_{\Upsilon_2}}{x_{\Upsilon_2}} \int dm^2_{\Upsilon_1} dm^2_{\Upsilon_2} \int dk_{x\Upsilon_1} dk_{y\Upsilon_1} dk_{x\Upsilon_2} dk_{y\Upsilon_2} \int \frac{dx_{\Upsilon\Upsilon}}{x_{\Upsilon\Upsilon}} \int dk_{x\Upsilon\Upsilon} dk_{y\Upsilon\Upsilon} dP_{\rm ibb7} \\ &\times \delta\left(\frac{m^2_{T,\Upsilon_1}}{x_{\Upsilon_1}} - \frac{m^2_{T4}}{x_4} - \frac{m^2_{T5}}{x_5}\right)\delta(k_{x4} + k_{x5} - k_{x\Upsilon_1})\delta(k_{y4} + k_{y5} - k_{y\Upsilon_1})\delta(x_{\Upsilon_1} - x_4 - x_5) \\ &\times \delta\left(\frac{m^2_{T,\Upsilon_2}}{x_{\Upsilon_2}} - \frac{m^2_{T6}}{x_6} - \frac{m^2_{T7}}{x_7}\right)\delta(k_{x6} + k_{x7} - k_{x\Upsilon_2})\delta(k_{y6} + k_{y7} - k_{y\Upsilon_2})\delta(x_{\Upsilon_2} - x_6 - x_7) \\ &\times \delta\left(\frac{M^2_{T,\Upsilon\Upsilon}}{x_{\Upsilon\Upsilon}} - \frac{m^2_{T,\Upsilon_1}}{x_{\Upsilon_1}} - \frac{m^2_{T,\Upsilon_2}}{x_{\Upsilon_2}}\right)\delta(k_{x\Upsilon_1} + k_{x\Upsilon_2} - k_{x\Upsilon\Upsilon})\delta(k_{y\Upsilon_1} + k_{y\Upsilon_2} - k_{y\Upsilon\Upsilon})\delta(x_{\Upsilon\Upsilon} - x_{\Upsilon_1} - x_{\Upsilon_2}), \end{aligned} \tag{12}$$

where $dP_{\rm ibb7}$ is taken from Eq. (7). The pair mass distributions require integration over the invariant mass of each Υ, $2m_b < m_{T\Upsilon} < 2m_B$, including its momentum fraction, x_Υ, and its transverse momenta, as well as integration over the x and k_T of the pair itself. The delta functions insure conservation of momentum for both Υ mesons and the $\Upsilon\Upsilon$ pair.

Figure 3 shows the predictions for the $\Upsilon\Upsilon$ pair mass distributions. All distributions are normalized to unity. Without any k_T dependence, the pair mass distribution is strongly peaked at the $4m_b$ threshold. The k_T dependence smears out the pair distribution, increasing $\langle M_{\Upsilon\Upsilon} \rangle$ by several GeV. The chosen default values of the transverse momentum range, $k_q^{\rm max} = 0.2$ GeV and $k_b^{\rm max} = 1.0$ GeV, as also assumed for light quarks and charm quarks respectively in a five-particle proton Fock state for J/ψ production [49]. In addition, the k_Υ integration range also is required to calculate the Υ pair mass distribution. The value $k_\Upsilon^{\rm max} = 1$ GeV is used as a default for both the Υ k_T range as well as that for the Υ pair. The pair mass distributions for $m_b = 4.65$ GeV, the bottom quark mass used in bottom quark calculations at next-to-leading order [23], are shown in the solid curve of Fig. 3(a).

The mass threshold is well above the average Υ pair mass of 18.15 GeV reported by the ANDY Collaboration [11]. The average pair mass in all cases is greater than 20 GeV. Varying the transverse integration range by increasing (dot-dashed curve) or decreasing (dashed curve) the range by a factor of two does not change the mass threshold and alters the average pair mass by less than 0.5 GeV, see the results labeled Set 1 on the left-hand side of Table I.

The pair mass obtained with the 1S value of m_b is much higher than the ANDY result. The lower value of the bottom quark mass, 4 GeV, used with the same set of transverse momentum integration ranges, does result in a lower average mass, as shown in Fig. 3(b). Even though the threshold is reduced and the average pair mass is decreased to ≈ 19 GeV, see the upper results on the right-hand side of

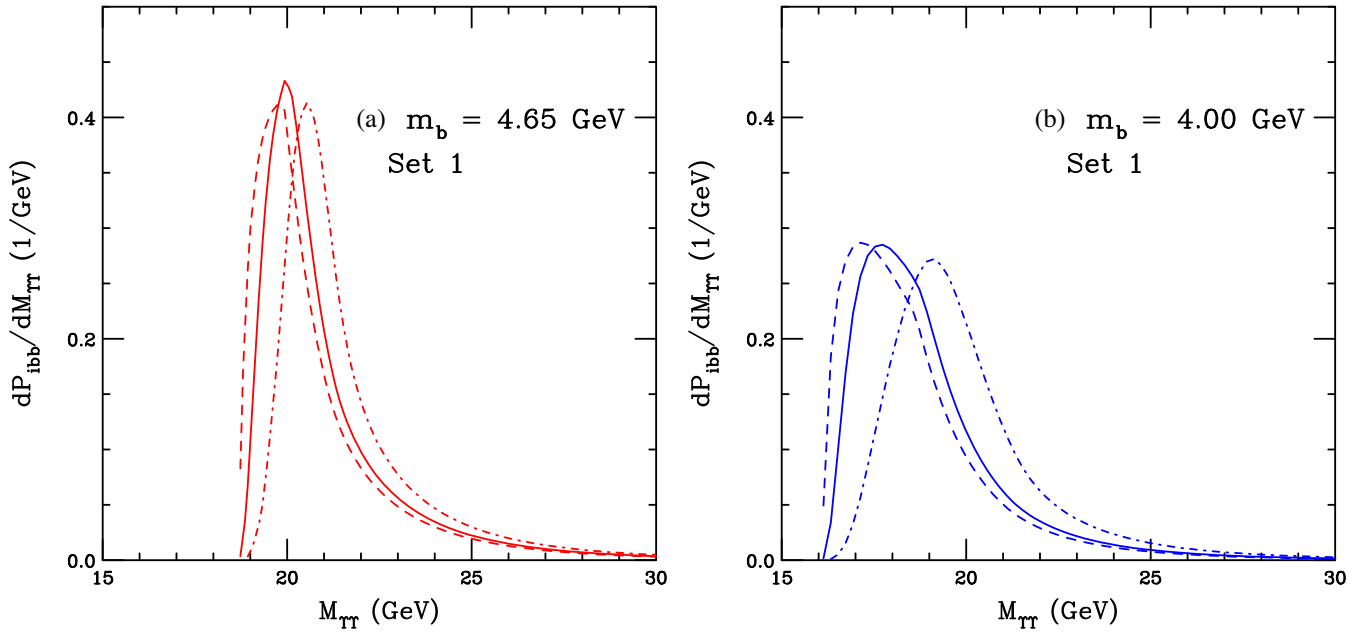

FIG. 3. The probability for double Υ production from a seven-particle Fock state as a function of the pair mass for three different k_T integration ranges, corresponding to Set 1 in Table I, are shown: $k_q^{\max} = 0.2$ GeV, $k_b^{\max} = 1.0$ GeV and $k_\Upsilon^{\max} = 1.0$ GeV (solid); $k_q^{\max} = 0.1$ GeV, $k_b^{\max} = 0.5$ GeV and $k_\Upsilon^{\max} = 0.5$ GeV (dashed); and $k_q^{\max} = 0.4$ GeV, $k_b^{\max} = 2.0$ GeV and $k_\Upsilon^{\max} = 2.0$ GeV (dot-dashed). All distributions are normalized to unity. In (a) $m_b = 4.65$ GeV while in (b) $m_b = 4.0$ GeV.

Table I, these values are still higher than obtained by the ANDY Collaboration.

In Ref. [26], predictions for double Υ production from the seven-particle Fock state were given assuming $m_{Tb} = 4.6$ GeV. (In that work, only averages were reported, no distributions were presented, and no systematic studies of the mass and transverse momentum were carried out.) It was found that the single Υ and $\Upsilon\Upsilon$ pair x distributions were similar to the equivalent $J/\psi J/\psi$ distributions. The average mass, $\langle M_{\Upsilon\Upsilon}\rangle$, was found to be 21.7 GeV for a proton beam, a few GeV above the two Υ mass threshold, $2m_\Upsilon = 18.9$ GeV. These results are in good agreement with the central value obtained for $m_b = 4.65$ GeV shown in Fig. 3(a) and in Table I.

The Υ pair mass distributions are quite sensitive to the range of k_T integration. Results for other values of $k_q^{\max}$,

TABLE I. The average Υ pair mass for given values of the bottom quark mass and the maximum range of k_T integration for light quarks, bottom quarks, and the Υ state.

	$m_b = 4.65$ GeV				$m_b = 4.00$ GeV			
Set	$k_q^{\max}$ (GeV)	$k_b^{\max}$ (GeV)	$k_\Upsilon^{\max}$ (GeV)	$\langle M_{\Upsilon\Upsilon}\rangle$ (GeV)	$k_q^{\max}$ (GeV)	$k_b^{\max}$ (GeV)	$k_\Upsilon^{\max}$ (GeV)	$\langle M_{\Upsilon\Upsilon}\rangle$ (GeV)
	0.2	1.0	1.0	21.02	0.2	1.0	1.0	18.96
1	0.1	0.5	0.5	20.74	0.1	0.5	0.5	18.59
	0.4	2.0	2.0	21.60	0.4	2.0	2.0	19.98
	0.2	1.0	2.0	21.37	0.2	1.0	2.0	19.47
2	0.1	0.5	1.0	20.87	0.1	0.5	1.0	18.76
	0.4	2.0	4.0	22.12	0.4	2.0	4.0	20.82
	0.2	2.0	2.0	21.59	0.2	2.0	2.0	19.98
3	0.1	1.0	1.0	21.02	0.1	1.0	1.0	18.95
	0.4	4.0	4.0	22.56	0.4	4.0	4.0	21.33
	0.2	1.0	5.0	22.10	0.2	1.0	5.0	21.01
4	0.1	0.5	2.5	21.49	0.1	0.5	2.5	19.62
	0.4	2.0	10.0	22.68	0.4	2.0	10.0	22.04
	0.2	2.0	5.0	22.32	0.2	2.0	5.0	21.17
5	0.1	1.0	2.5	21.56	0.1	1.0	2.5	19.77
	0.4	4.0	10.0	23.88	0.4	4.0	10.0	22.98

$k_b^{\max}$ and $k_\Upsilon^{\max}$ are shown for both values of m_b considered. Sets 2 through 5 in Table I give the average Υ pair mass for each central value as well as for halving and doubling the ranges for each chosen central value. Note that the central value of $k_q^{\max}$ is always 0.2 GeV. The central value of $k_b^{\max}$ is varied from 1 to 2 GeV and, finally, the central value of $k_\Upsilon^{\max}$ is either 1, 2 or 5 GeV. The value of $k_b^{\max}$ is assumed to be either less than or equal to $k_\Upsilon^{\max}$, never larger.

The larger the upper limit of the range of integration over momentum, the larger the average pair mass becomes. The bottom quark mass obtained from the $\Upsilon(1S)$, $m_b = 4.65$ GeV, gives a consistently higher mass of the double Υ state, always greater than 20 GeV. On the other hand, the lower limit chosen for the b quark mass, 4 GeV, results in a smaller Υ pair mass, as low as 18.6 GeV, but still larger than the average Υ pair mass reported by ANDY.

The pair mass distributions are shown in Figs. 4 and 5 from Sets 2-5 of k_T integration ranges in Table I. The central values, the first line of each set in the table, are

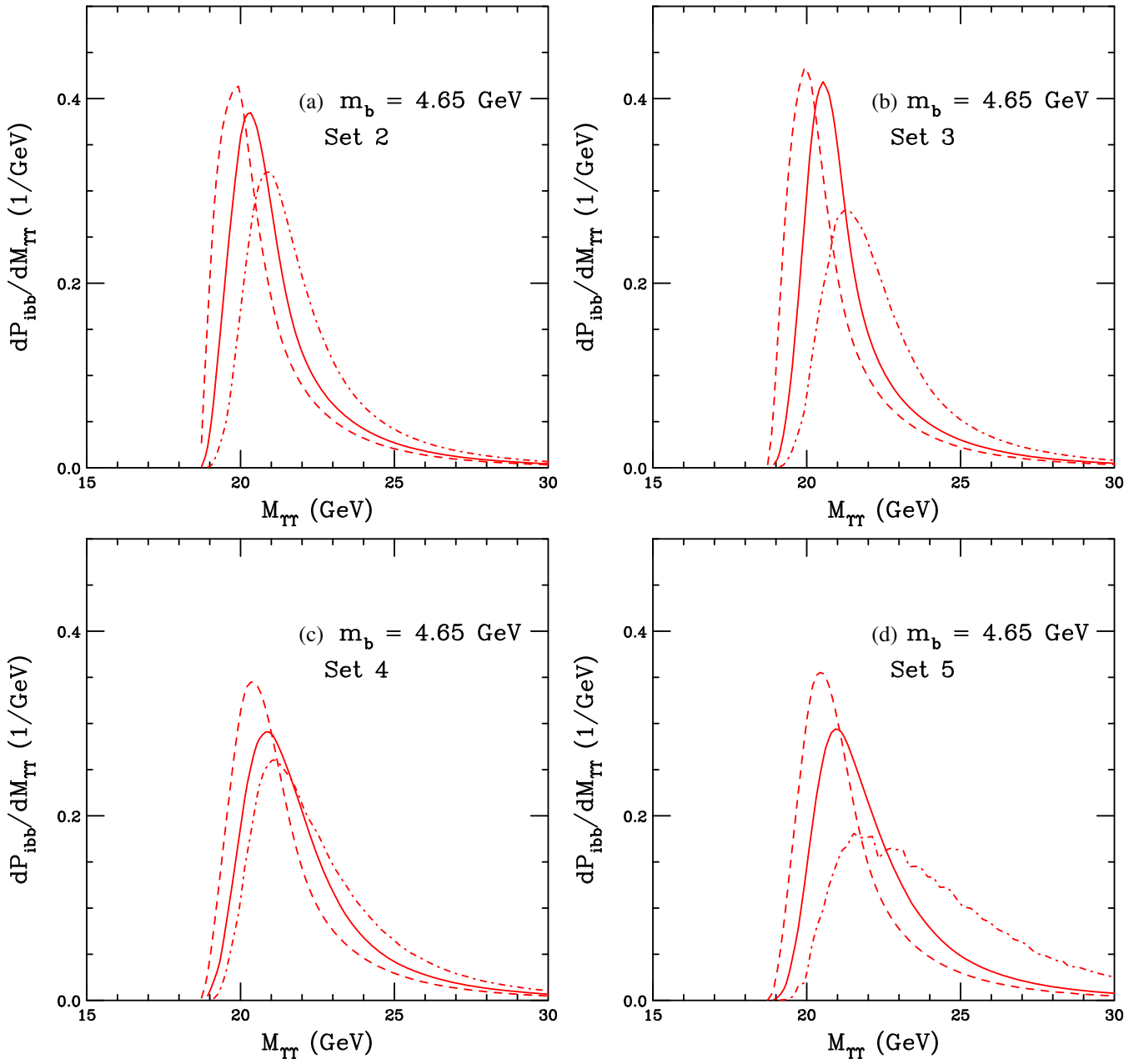

FIG. 4. The double Υ pair mass distribution normalized to unity from a seven-particle proton Fock state with $m_b = 4.65$ GeV. Different k_T integration ranges, corresponding to Sets 2-5 of Table I, are shown in (a)-(d) respectively. In each case, the solid curve shows the calculation for the central value of the range while the dashed and dot-dashed curves show half and double the central value of the ranges respectively.

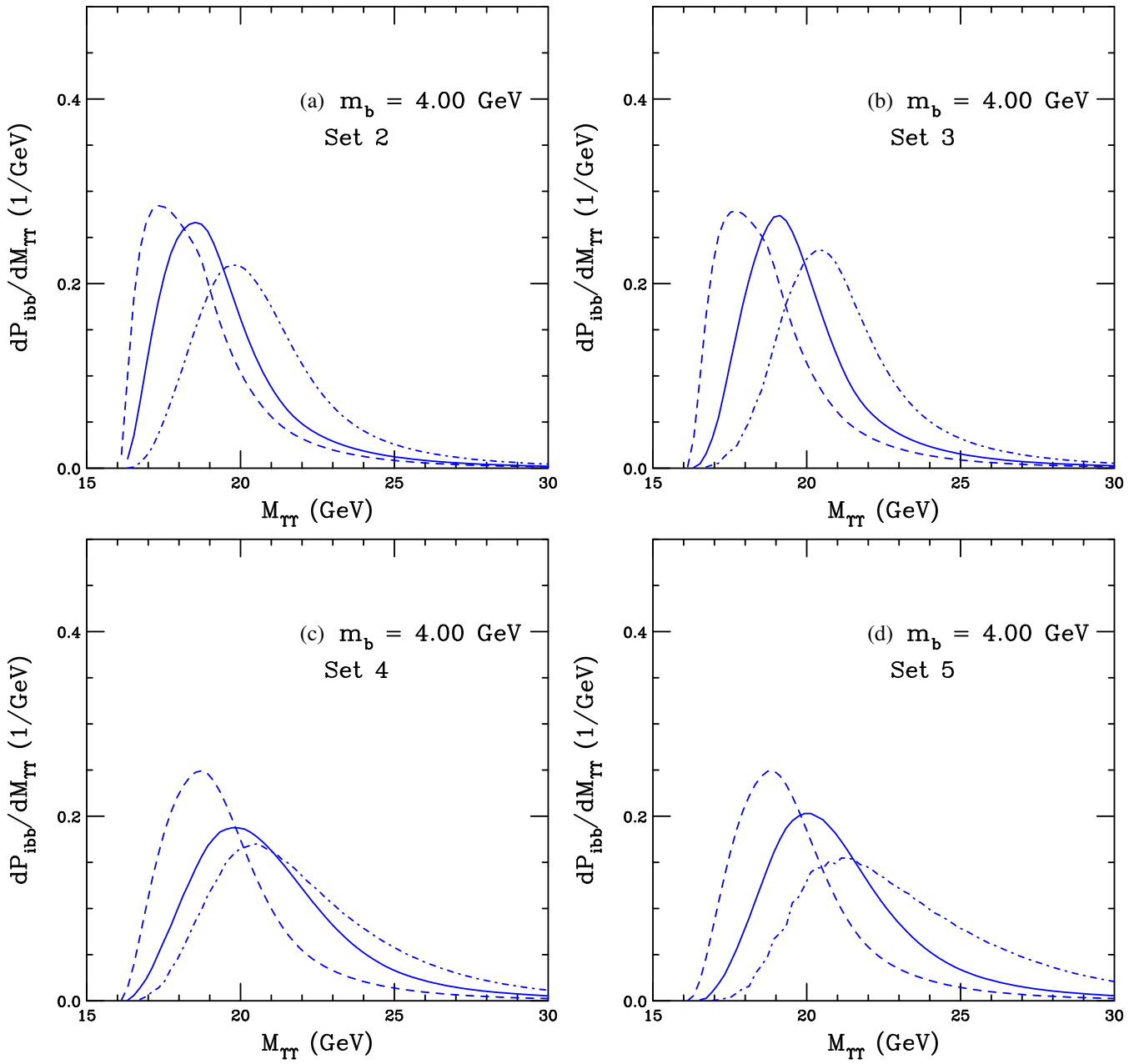

FIG. 5. The double Υ pair mass distribution normalized to unity from a seven-particle proton Fock state with $m_b = 4.00$ GeV. Different k_T integration ranges, corresponding to Sets 2-5 of Table I, are shown in (a)-(d) respectively. In each case, the solid curve shows the calculation for the central value of the range while the dashed and dot-dashed curves show half and double the central value of the ranges respectively.

shown by the solid curves while the dashed curve shows the result for the integration range reduced by half and the dot-dashed curve presents the results for doubling the k_T integration range. All distributions are normalized to unity. It is clear that not just the average pair mass increases with the integration range in k_T but also the width of the distribution. In cases where half the integration range is taken (dashed curves), the width is narrower while, when the integration range is doubled (dot-dashed curves), the distributions are broader.

None of the results presented here are compatible with the ANDY results. Indeed, increasing the integration range does not affect the threshold and effectively only serves to increase the pair mass. Unlike the earlier NA3 results on double J/ψ production, where the pair mass was well above twice the J/ψ mass, the ANDY Collaboration reports an average pair mass *below* twice the mass of a single $\Upsilon(1S)$ state, 18.92 GeV. Assuming $m_b = 4$ GeV in the $b\bar{b}$ pair mass integration, it is possible to obtain a pair mass below $2m_\Upsilon$ but this seems unlikely, especially since it

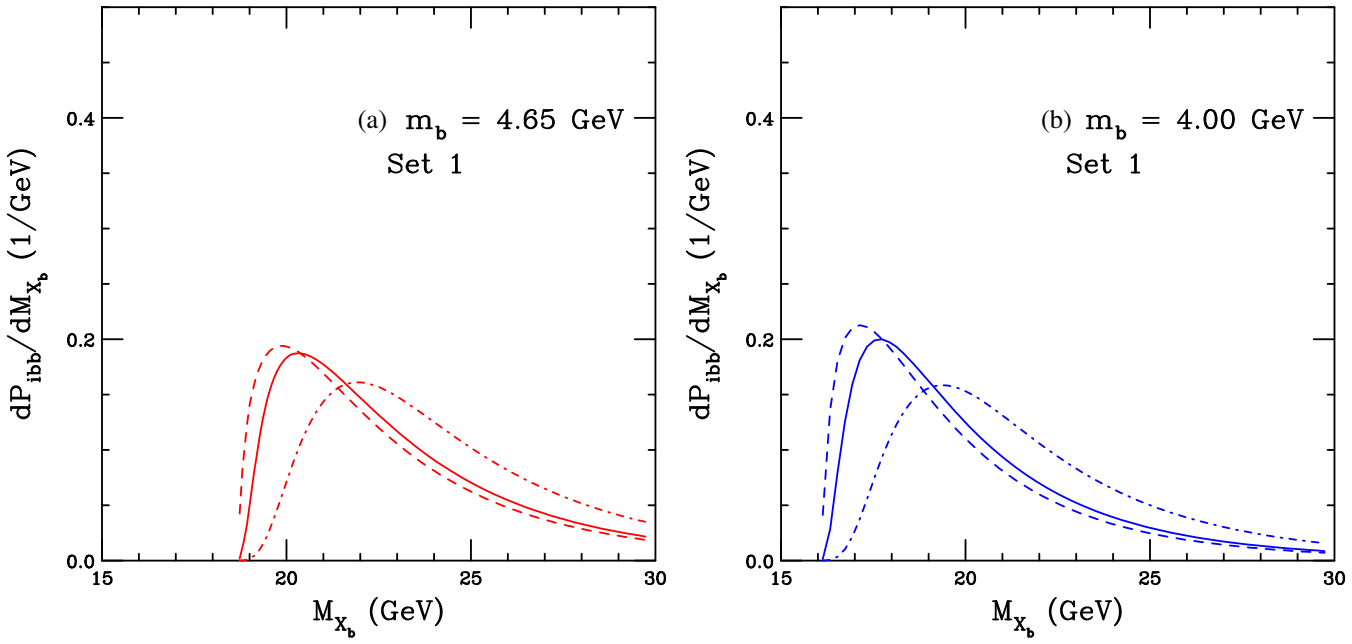

FIG. 6. The probability for X_b production from a seven-particle Fock state as a function of the X_b mass for three different k_T integration ranges, corresponding to Set 1 in Table II, are shown: $k_q^{\max} = 0.2$ GeV, different k_T integration ranges are shown: $k_q^{\max} = 0.2$ GeV, $k_b^{\max} = 1.0$ GeV and $k_{X_b}^{\max} = 1.0$ GeV (solid); $k_q^{\max} = 0.1$ GeV, $k_b^{\max} = 0.5$ GeV and $k_{X_b}^{\max} = 0.5$ GeV (dashed); and $k_q^{\max} = 0.4$ GeV, $k_b^{\max} = 2.0$ GeV and $k_{X_b}^{\max} = 2.0$ GeV (dot-dashed). All distributions are normalized to unity. In (a) $m_b = 4.65$ GeV while in (b) $m_b = 4.0$ GeV.

is obtained with a particularly low bottom quark mass, less than what is generally assumed for the current bottom quark mass. Indeed, in calculations of uncertainty bands on perturbative bottom quark production such as in FONLL [56], the b quark mass range is $4.5 \le m_b \le 5$ GeV.

It is noteworthy, however, that the average calculated pair masses, for Set 1 and $m_b = 4$ GeV, as in Fig. 3(b), are relatively compatible with the models of X_b masses. The next section considers the effects on the distributions reported here if the internal kinematics of the Fock state assumes a single tetraquark configuration of $b\bar{b}b\bar{b}$ not directly bound in an Υ pair.

C. X_b tetraquark production from a $|uudb\bar{b}b\bar{b}\rangle$ state

The restriction of two $\Upsilon(1S)$ states produced from the $|uudb\bar{b}b\bar{b}\rangle$ Fock state is lifted in this section to determine whether a direct X_b configuration, without the assumption of two bound $\Upsilon(1S)$ states, might be more compatible with the reported ANDY mass distribution.

The same starting point, Eq. (7), is assumed. Now, however, the x_F distribution is calculated with the addition of a single longitudinal delta function, $\delta(x_{X_b} - x_4 - x_5 - x_6 - x_7)$. Despite the rearrangement of the bottom quarks in this configuration, the M_{X_b} x_F distribution is identical to the one for the Υ pair shown in the dashed curve in Fig. 2(a). This suggests that the longitudinal distributions are independent of any correlations between the partons in the state as long as the same number and type of partons are included.

Next, the mass distributions are calculated, without including the pair mass constraints, $2m_b < m_{T\Upsilon} < 2m_B$, in Eq. (12). The X_b mass distribution is then

$$\frac{dP_{\rm ibb7}}{dM_{X_b}^2} = \int \frac{dx_{X_b}}{x_{X_b}} \int dk_{xX_b} dk_{yX_b} dP_{\rm ibb7} \delta\left(\frac{M_{T,X_b}^2}{x_{X_b}} - \frac{m_{T,4}^2}{x_4} - \frac{m_{T,5}^2}{x_5} - \frac{m_{T,6}^2}{x_6} - \frac{m_{T,7}^2}{x_7}\right) \times \delta(k_{x4} + k_{x5} + k_{x6} + k_{x7} - k_{xX_b}) \delta(k_{y4} + k_{y5} + k_{y6} + k_{y7} - k_{yX_b}) \delta(x_{X_b} - x_4 - x_5 - x_6 - x_7), \quad (13)$$

where $dP_{\rm ibb7}$ is from Eq. (7).

The mass distributions for the X_b from Eq. (13) are shown in Fig. 6 for the same values of m_b, $k_q^{\max}$ and $k_b^{\max}$ as shown in Fig. 3 (Set 1 in Table II). In this case the k_T range for the X_b is taken to be the same as for the b quarks. The results here are also normalized to unity.

The mass distributions are much broader than those in Fig. 3, even though they have the same thresholds. They

TABLE II. The average X_b mass for given values of the bottom quark mass and the maximum range of k_T integration for light quarks, bottom quarks, and the X_b.

	$m_b = 4.65$ GeV				$m_b = 4.00$ GeV			
Set	$k_q^{\max}$ (GeV)	$k_b^{\max}$ (GeV)	$k_{X_b}^{\max}$ (GeV)	$\langle M_{X_b}\rangle$ (GeV)	$k_q^{\max}$ (GeV)	$k_b^{\max}$ (GeV)	$k_{X_b}^{\max}$ (GeV)	$\langle M_{X_b}\rangle$ (GeV)
	0.2	1.0	1.0	22.66	0.2	1.0	1.0	20.11
1	0.1	0.5	0.5	22.31	0.1	0.5	0.5	19.65
	0.4	2.0	2.0	23.72	0.4	2.0	2.0	21.47

become broader because there is no integration over the Υ mass in this case, as in Eq. (12), where the Υ mass was restricted to be between $2m_b$ and $2m_B$. These broader distributions result in higher average masses for the X_b, typically 1–2 GeV higher than for the same Fock state where the $b\bar{b}b\bar{b}$ is considered to be bound into an Υ pair. Thus, no further systematic studies of the mass dependence on $k^{\max}$ are considered here. The average X_b masses from these calculations are given in Table II, corresponding to the first three rows of Table I.

It is worth noting that the probability for an X_b state could be considerably different from that of a double Υ state. The factors of F_B for Υ production, as in Eq. (9), would be replaced by a single factor F_{X_b}, giving

$$\sigma_{\rm ibb7}^{X_b}(pp) = F_{X_b}\frac{P_{\rm ibb7}^0}{P_{\rm ib5}^0}\sigma_{\rm ib5}(pp). \tag{14}$$

In the CEM, F_B is determined by a fit to Υ production data. Since not all bottom tetraquark states have so far been reported, aside from the ANDY result which did not determine a cross section, the extraction of F_{X_b} is not yet possible.

Finally, one could consider a tetraquark to be produced as a single massive object rather than composed of two individual $b\bar{b}$ pairs. In such a case, the tetraquark could be assumed to be produced in a four-particle Fock state, $|uudX_b\rangle$, similar to a massive gluon. However, this configuration does not have a mass threshold and would carry a lower share of the nucleon momentum on average, $\langle x_{X_b}\rangle \sim 0.5$ as long as $\hat{M}_{X_b} \gg \hat{m}_q$. Thus this type of state would not conform to the kinematic criteria required for either a double Υ state or an $X_b(b\bar{b}b\bar{b})$ state.

III. SUMMARY

The ANDY Collaboration suggests that they have produced a tetraquark $b\bar{b}b\bar{b}$ state with an average mass of 18.15 GeV [11]. The calculations for Υ pair and X_b production from a seven-particle double intrinsic bottom state presented here are incompatible with the low mass suggested from the ANDY data. However, the assumption of a double Υ state produced from a seven-particle $|uudb\bar{b}b\bar{b}\rangle$ state is compatible with previously predicted tetraquark masses and could be considered a source of tetraquark production via a double $\Upsilon(1S)$ state.

ACKNOWLEDGMENTS

R. V. would like to thank S. J. Brodsky and V. Cheung for discussions. This work was performed under the auspices of the U.S. Department of Energy by Lawrence Livermore National Laboratory under Contract No. DE-AC52-07NA27344 and the LLNL-LDRD Program under Project No. 21-LW-034.

[1] M. Gell-Mann, A schematic model of baryons and mesons, Phys. Lett. **8**, 214 (1964).
[2] S. K. Choi *et al.* (Belle Collaboration), Observation of a Narrow Charmonium-Like State in Exclusive $B^{\pm} \to K^{\pm}\pi^{+}\pi^{-}J/\psi$ Decays, Phys. Rev. Lett. **91**, 262001 (2003).
[3] A. M. Sirunyan *et al.* (CMS Collaboration), Evidence for $X(3872)$ in PbPb collisions and studies of its prompt production at $\sqrt{s_{\rm NN}} = 5.02$ TeV, arXiv:2102.13048.
[4] S. K. Choi *et al.* (Belle Collaboration), Observation of a Resonance-Like Structure in the $pi^{\pm}\psi'$ Mass Distribution in Exclusive $B \to K\pi^{\pm}\psi'$ Decays, Phys. Rev. Lett. **100**, 142001 (2008).
[5] R. Aaij *et al.* (LHCb Collaboration), Observation of the Resonant Character of the $Z(4430)^-$ State, Phys. Rev. Lett. **112**, 222002 (2014).
[6] M. Ablikim *et al.* (BESIII Collaboration), Observation of a Charged Charmoniumlike Structure in $e^+e^- \to \pi^+\pi^- J/\psi$ at $\sqrt{s} = 4.26$ GeV, Phys. Rev. Lett. **110**, 252001 (2013).
[7] Z. Q. Liu *et al.* (Belle Collaboration), Study of $e^+e^- \to \pi^+\pi^- J/\psi$ and Observation of a Charged Charmoniumlike State at Belle, Phys. Rev. Lett. **110**, 252002 (2013); Erratum, Phys. Rev. Lett. **111**, 019901 (2013).
[8] R. Aaij *et al.* (LHCb Collaboration), Observation of structure in the J/ψ pair mass spectrum, Sci. Bull. **65**, 1983 (2020).

[9] R. Aaij *et al.* (LHCb Collaboration), Observation of a Narrow Pentaquark State, $P_c(4312)^+$, and of Two-Peak Structure of the $P_c(4450)^+$, Phys. Rev. Lett. **122**, 222001 (2019).

[10] A. Garmash *et al.* (Belle Collaboration), Observation of $Z_b(10610)$ and $Z_b(10650)$ Decaying to B Mesons, Phys. Rev. Lett. **116**, 212001 (2016).

[11] L. C. Bland *et al.* (ANDY Collaboration), Observation of Feynman scaling violations and evidence for a new resonance at RHIC, arXiv:1909.03124.

[12] M. Karliner, J. L. Rosner, and S. Nussinov, $QQ\bar{Q}\,\bar{Q}$ states: Masses, production and decays, Phys. Rev. D **95**, 034011 (2017).

[13] Z.-G. Wang, Analysis of the $QQ\bar{Q}\,\bar{Q}$ tetraquark states with QCD sum rules, Eur. Phys. J. C **77**, 432 (2017).

[14] Y. Bai, S. Lu, and J. Osborne, Beauty-full tetraquarks, Phys. Lett. B **798**, 134930 (2019).

[15] J. Wu, Y.-R. Liu, K. Chen, X. Liu, and S.-L. Zhu, Heavy-flavored tetraquark states with the $QQ\bar{Q}\,\bar{Q}$ configuration, Phys. Rev. D **97**, 094015 (2018).

[16] G. Yang, J. Ping, L. He, and Q. Wang, Potential model prediction of fully-heavy tetraquarks $QQ\bar{Q}\,\bar{Q}$ ($Q = c$, b), arXiv:2006.13756.

[17] X. Z. Weng, X. L. Chen, W. Z. Deng, and S. L. Zhu, Systematics of fully heavy tetraquarks, Phys. Rev. D **103**, 034001 (2021).

[18] C. Hughes, E. Eichten, and C. T. H. Davies, Searching for beauty-fully bound tetraquarks using lattice nonrelativistic QCD, Phys. Rev. D **97**, 054505 (2018).

[19] J.-M. Richard, A. Valcance, and J. Vijande, String dynamics and metastability of all-heavy tetraquarks, Phys. Rev. D **95**, 054019 (2017).

[20] R. Aaij *et al.* (LHCb Collaboration), Search for beautiful tetraquarks in the $\Upsilon(1S)\mu^+\mu^-$ invariant mass spectrum, J. High Energy Phys. 10 (2018) 086.

[21] Albert M. Sirunyan *et al.* (CMS Collaboration), Measurement of the $\Upsilon(1S)$ pair production cross section and search for resonances decaying to $\Upsilon(1S)\mu^+\mu^-$ in proton-proton collisions at $\sqrt{s} = 13$ TeV, Phys. Lett. B **808**, 135578 (2020).

[22] R. Aaij *et al.* (LHCb Collaboration), Study of $b\bar{b}$ correlations in high energy proton-proton collisions, J. High Energy Phys. 11 (2017) 030.

[23] R. Vogt, $b\bar{b}$ kinematic correlations in cold nuclear matter, Phys. Rev. C **101**, 024910 (2020).

[24] J. Badier *et al.* (NA3 Collaboration), Evidence for $\psi\psi$ production in π^- interactions at 150 GeV/c and 280 GeV/c, Phys. Lett. **114B**, 457 (1982).

[25] J. Badier *et al.* (NA3 Collaboration), $\psi\psi$ Production and limits on beauty meson production from 400 GeV/c protons, Phys. Lett. **158B**, 85 (1985).

[26] R. Vogt and S. J. Brodsky, Intrinsic charm contribution to double quarkonium hadroproduction, Phys. Lett. B **349**, 569 (1995).

[27] R. Vogt, QCD mechanisms for double quarkonium and open heavy meson hadroproduction, Nucl. Phys. **B446**, 159 (1995).

[28] S. J. Brodsky, P. Hoyer, C. Peterson, and N. Sakai, The intrinsic charm of the proton, Phys. Lett. **93B**, 451 (1980).

[29] S. J. Brodsky, C. Peterson, and N. Sakai, Intrinsic heavy quark states, Phys. Rev. D **23**, 2745 (1981).

[30] R. Vogt, S. J. Brodsky, and P. Hoyer, Systematics of charm production, Nucl. Phys. **B383**, 643 (1992).

[31] R. Vogt and S. J. Brodsky, Charmed hadron asymmetries in the intrinsic charm coalescence model, Nucl. Phys. **B478**, 311 (1996).

[32] T. Gutierrez and R. Vogt, Leading charm in hadron nucleus interactions in the intrinsic charm model, Nucl. Phys. **B539**, 189 (1999).

[33] S. J. Brodsky, P. Hoyer, A. H. Mueller, and W.-K. Tang, New QCD production mechanisms for hard processes at large x, Nucl. Phys. **B369**, 519 (1992).

[34] S. Paiva, M. Nielsen, F. S. Navarra, F. O. Duraes, and L. L. Barz, Virtual meson cloud of the nucleon and intrinsic strangeness and charm, Mod. Phys. Lett. A **13**, 2715 91998).

[35] M. Neubert, Heavy quark symmetry, Phys. Rep. **245**, 259 (1994).

[36] F. M. Steffens, W. Melnitchouk, and A. W. Thomas, Charm in the nucleon, Eur. Phys. J. C **11**, 673 (1999).

[37] T. J. Hobbs, J. T. Londergan, and W. Melnitchouk, Phenomenology of nonperturbative charm in the nucleon, Phys. Rev. D **89**, 074008 (2014).

[38] J. Pumplin, H. L. Lai, and W. K. Tung, The charm parton content of the nucleon, Phys. Rev. D **75**, 054029 (2007).

[39] P. M. Nadolsky *et al.*, Implications of CTEQ global analysis for collider observables, Phys. Rev. D **78**, 013004 (2008).

[40] S. Dulat *et al.*, Intrinsic charm parton distribution functions from CTEQ-TEA global analysis, Phys. Rev. D **89**, 073004 (2014).

[41] P. Jimenez-Delgado, T. J. Hobbs, J. T. Londergan, and W. Melnitchouk, New Limits on Intrinsic Charm in the Nucleon from Global Analysis of Parton Distributions, Phys. Rev. Lett. **114**, 082002 (2015).

[42] R. D. Ball *et al.* (NNPDF Collaboration), A determination of the charm content of the proton, Eur. Phys. J. C **76**, 647 (2016).

[43] J. Blümlein, A kinematic condition on intrinsic charm, Phys. Lett. B **753**, 619 (2016).

[44] S. J. Brodsky, A. Kusina, F. Lyonnet, I. Schienbein, H. Spiesberger, and R. Vogt, A review of the intrinsic heavy quark content of the nucleon, Adv. High Energy Phys. **2015**, 231547 (2015).

[45] S. J. Brodsky, G. I. Lykasov, A. V. Lipatov, and J. Smiesko, Novel heavy-quark physics phenomena, Prog. Part. Nucl. Phys. **114**, 103802 (2020).

[46] R. S. Sufian, T. Liu, A. Alexandru, S. J. Brodsky, G. F. de Téramond, H. G. Dosch, T. Draper, K. F. Liu, and Y. B. Yang, Constraints on charm-anticharm asymmetry in the nucleon from lattice QCD, Phys. Lett. B **808**, 135633 (2020).

[47] E. Norrbin and R. Vogt, Bottom production asymmetries at the LHC, arXiv:hep-ph/0003056.

[48] R. Vogt and S. J. Brodsky, QCD and intrinsic heavy quark predictions for leading charm and beauty hadroproduction, Nucl. Phys. **B438**, 261 (1995).

[49] R. Vogt, Limits on intrinsic charm production from the SeaQuest experiment, Phys. Rev. C **103**, 035204 (2021).
[50] R. Vogt, S. J. Brodsky, and P. Hoyer, Systematics of J/ψ production, Nucl. Phys. **B360**, 67 (1991).
[51] R. Vogt, Shadowing effects on J/ψ and Υ production at energies available at the CERN Large Hadron Collider, Phys. Rev. C **92**, 034909 (2015).
[52] J. Badier *et al.* (NA3 Collaboration), Experimental J/ψ Hadronic Production from 150 GeV/c to 280 GeV/c, Z. Phys. C **20**, 101 (1983).
[53] R. E. Nelson, R. Vogt, and A. D. Frawley, Narrowing the uncertainty on the total charm cross section and its effect on the J/ψ cross section, Phys. Rev. C **87**, 014908 (2013).
[54] P. A. Zyla *et al.* (Particle Data Group), The review of particle physics (2021), Prog. Theor. Exp. Phys. (**2020**), 083C01 and (2021) update.
[55] R. Vogt, Heavy flavor azimuthal correlations in cold nuclear matter, Phys. Rev. C **98**, 034907 (2018).
[56] M. Cacciari, P. Nason, and R. Vogt, QCD Predictions for Charm and Bottom Production at RHIC, Phys. Rev. Lett. **95**, 122001 (2005).